Infarction of tumor vessels by NGR-peptide–directed targeting of tissue factor: experimental results and first-in-man experience

Ralf Bieker,[1] Torsten Kessler,[1] Christian Schwöppe,[1] Teresa Padró,[1] Thorsten Persigehl,[2] Christoph Bremer,[2] Johannes Dreischalück,[1] Astrid Kolkmeyer,[1] Walter Heindel,[2] *Rolf M. Mesters,[1] and *Wolfgang E. Berdel[1]

Departments of [1]Medicine/Hematology and Oncology and [2]Clinical Radiology, University of Muenster, Muenster, Germany

We induced thrombosis of blood vessels in solid tumors in mice by a fusion protein consisting of the extracellular domain of tissue factor (truncated tissue factor, tTF) and the peptide GNGRAHA, targeting aminopeptidase N (CD13) and the integrin $\alpha_v\beta_3$ (CD51/CD61) on tumor vascular endothelium. The designed fusion protein tTF-NGR retained its thrombogenic activity as demonstrated by coagulation assays. In vivo studies in mice bearing established human adenocarcinoma (A549), melanoma (M21), and fibrosarcoma (HT1080) revealed that systemic administration of tTF-NGR induced partial or complete thrombotic occlusion of tumor vessels as shown by histologic analysis. tTF-NGR, but not untargeted tTF, induced significant tumor growth retardation or regression in all 3 types of solid tumors. Thrombosis induction in tumor vessels by tTF-NGR was also shown by contrast enhanced magnetic resonance imaging (MRI). In the human fibrosarcoma xenograft model, MRI revealed a significant reduction of tumor perfusion by administration of tTF-NGR. Clinical first-in-man application of low dosages of this targeted coagulation factor revealed good tolerability and decreased tumor perfusion as measured by MRI. Targeted thrombosis in the tumor vasculature induced by tTF-NGR may be a promising strategy for the treatment of cancer. (Blood. 2009;113:5019-5027)

Introduction

An angiogenic phenotype is a characteristic feature of solid tumors,[1,2] and of some hematologic malignancies,[3,4] and an absolute requirement for tumor progression.[5,6] Molecules inhibiting angiogenesis or selectively targeting and destroying new blood vessels may be promising agents for the treatment of tumors.[7,8] Denying a tumor its blood supply can dramatically reduce tumor growth, and in some experiments, even eradicate the tumor.[7,9] Antiangiogenic therapies interfere with the complex processes of growth, migration, and differentiation of blood vessels. In contrast, vascular targeting aims at the destruction of tumor blood vessels with the result of tumor infarction.[10,11]

Recently, novel approaches for cancer treatment based on targeting of the human coagulation-inducing protein tissue factor (TF) to tumor vasculature have been proposed.[10-12] TF, a transmembrane protein, is the main initiator of coagulation in vivo. A soluble mutant form of TF that lost its transmembrane domain (truncated TF, tTF) has almost no coagulation inducing activity.[13] By localizing tTF to the proximity of a phospholipid membrane (eg, tumor vascular endothelium), its potent coagulation activation is partly recovered.[10-12,14] Such a strategy using tTF has been reported by a few groups only. To this end, the specific targeting of tTF to tumor vasculature has been accomplished with antibodies and peptides directed against a variety of tumor vessel markers, including the ED-B domain of fibronectin,[10] prostate specific antigen,[14] vascular cell adhesion molecule (VCAM-1),[11] MHC class II,[12] and integrins such as $\alpha_v\beta_3$.[15] In all of these studies, tTF homed to tumor vessels and rapidly induced thrombosis.

Recent studies revealed that small peptides comprising the NGR-motif bound strictly to the endothelium of angiogenic blood vessels.[8,16,17] Furthermore, it has been demonstrated that a binding site for NGR peptides on tumor vasculature is aminopeptidase N (APN; CD13). The expression of CD13 is up-regulated in endothelial cells within mouse and human tumors. Moreover, in tissues that undergo angiogenesis blood vessels express CD13. Beside the angiogenic compartment, CD13 coincides with commitment to the myeloid lineage and is expressed on the normal and leukemic progeny of myeloid cells within the hematopoietic compartment.[18-20] Recently, a study showed that drugs containing the NGR motif differentially bound CD13. CD13 expressed on tumor vasculature could function as a binding site for the NGR motif, whereas CD13 expressed in normal kidney and in myeloid cells failed to bind to a fusion protein composed of the NGR motif and tumor necrosis factor.[21] Furthermore, NGR can rapidly convert to isoaspartate-glycine-arginine (*iso*DGR) by asparagine deamidation, generating $\alpha_v\beta_3$ ligands.[22] The implication of this study is that the tumor-targeting properties of NGR-drug conjugates rely on recognition of a CD13 isoform and $\alpha_v\beta_3$ preferentially expressed within tumor associated vessels.

In our study, we generated the fusion protein tTF-NGR consisting of tTF and a small NGR-peptide coupled to the C-terminal region of tTF, thus targeting tumor endothelial cells. tTF-NGR effectively inhibited tumor growth in mice by thrombotic occlusion of tumor vessels without any major side effects in other organs and showed inhibition of tumor perfusion in the first patients treated with this molecule.

Methods

Cloning, expression, and purification of tTF and tTF-NGR

The cDNA encoding tTF containing amino acids 1-218 and tTF-GNGRAHA, in which the heptapeptide is linked to the C-terminus of tTF (tTF-NGR), was

Submitted April 11, 2008; accepted December 3, 2008. Prepublished online as *Blood* First Edition paper, January 28, 2009; DOI 10.1182/blood-2008-04-150318.

*R.M.M. and W.E.B. contributed equally and share senior authorship.

An Inside *Blood* analysis of this article appears at the front of this issue.

The publication costs of this article were defrayed in part by page charge payment. Therefore, and solely to indicate this fact, this article is hereby marked "advertisement" in accordance with 18 USC section 1734.

amplified by polymerase chain reaction (PCR) using the primers 5′-CATGCCATGGGATCAGGCACTACAAATACTGTGGCAGCATATAAT-3′ (5′-primer), 5′-CGGGATCCTATTATCTGAATTCCCCTTTCTCCTGGCCCAT-3′ (3′-primer) for tTF, and 5′-CATGCCATGGGATCAGGCACTACAAATACTGTGGCAGCATATAAT-3′ (5′-primer), 5′-CGGGATCCTATTATGCATGTGCTCTTCCGTTACCTCTGAATTCCCC-3′ (3′-primer) for tTF-NGR. With the DNA-Ligation Kit (Novagen, Schwalbach am Taunus, Germany), the cDNA was cloned into the expression vector pET-30(+)a (Novagen) using the *Bam*HI and *Nco*I sites of the vector.

The vectors were introduced in competent *Escherichia coli* cells (BL21 DE3) according to the manufacturer's protocol (Novagen). After stimulating with IPTG (Novagen), the cells were harvested and 5 to 7 mL lysis buffer (10 mM Tris-HCl, pH 7.5; 150 mM NaCl; 1 mM $MgCl_2$; 10 μg/mL aprotinin; and 2 mg/mL lysozyme) per gram wet weight and 20 μL benzonase (Novagen) were added to the pellet. Then the cells were incubated for 90 minutes at room temperature (RT) and centrifuged at 12 000*g* for 20 minutes at 4°C. The pellet was resuspended and homogenized by sonication in washing buffer (10 mM Tris/HCl, pH 7.5; 1 mM EDTA [ethylenediaminetetraacetic acid], 3% Triton X-100). To solubilize the inclusion bodies, 2 to 4 mL Guanidinium buffer (6 M GuCl, 0.5 M NaCl, 20 mM NaH_2PO_4, 1 mM dithiothreitol [DTT]) per gram wet weight was added. After incubation overnight at RT, the suspension was centrifuged at 5000 × *g* for 30 minutes at 4°C. The supernatant was filtered through a 0.22-μm filter and loaded onto a nitrilotriacetic acid column (Ni-NTA; Novagen). Purification and refolding was done with the His Bind Buffer Kit (Novagen) according to the manufacturer's protocol. To remove the salt, the suspension was dialyzed in a Slide-A-Lyzer^R 10 K dialysis cassette (Pierce, Bonn, Germany) against Tris [tris(hydroxymethyl)aminomethane]-buffered saline (TBS) buffer (20 mM Tris, 150 mM NaCl, pH 7.4). Subsequently, tTF and tTF-NGR were analyzed under denaturing conditions by sodium dodecyl sulfate polyacrylamide gel electrophoresis (SDS-PAGE) and Western blot using mouse monoclonal anti–human tissue factor antibody (American Diagnostica, Pfungstadt, Germany; dilution 1:1000).

For clinical application, tTF-NGR was produced by a similar approach under good manufacturing practice (GMP)–like conditions using a multistep high-performance liquid chromatography (HPLC)–based purification process (HPLC unit: ÄKTA purifier 100 System; GE Healthcare, Uppsala, Sweden). Each sample produced was tested for purity and activity (including xenotransplantation mouse experiments) as described.

Factor X activation by tTF and tTF-NGR

The ability of tTF and tTF-NGR to enhance the specific proteolytic activation of factor (F) X by FVIIa was assessed as described by Ruf et al.[23] Briefly, to each well in a microtiter plate was added 20 μL of: (1) 50 nM recombinant FVIIa (Novo-Nordisc, Bagsværd, Denmark) in TBS–bovine serum albumin (BSA); (2) 0.16 nM to 1.6 μM tTF/tTF-NGR in TBS containing 0.1% BSA; or (3) 25 nM $CaCl_2$ and 500 μM phospholipids (phosphatidylcholine/phosphatidylserine, 70/30, MM; Sigma-Aldrich, München, Germany). After 10 minutes at RT, 20 μL of the substrate FX (Enzyme Research Laboratories, Swansea, United Kingdom) was added at a concentration of 5 μM. Aliquots were removed from the reaction mixture every minute and stopped in 100 nM EDTA. Spectrozyme FXa (American Diagnostica, Greenwich, CT) was added, and rates of FXa generation were monitored by the development of color at 405 nm with a microplate reader (Bio-Rad, Hercules, CA).

Binding studies

We applied flow cytometry using monoclonal antibodies (ABs) against CD13 (BD Biosciences, Heidelberg, Germany; phycoerythrin [PE]–linked) or $\alpha_v\beta_3$ (CD51/CD61; BD Pharmingen, Heidelberg, Germany; PE-linked), and thrombomodulin (Dako, Glostrup, Denmark) to test for presence of these molecules on human umbilical vein endothelial cells (HUVECs). Briefly, cells were blocked using human immunoglobulin (Ig) before incubation with the AB or isotype-matched control antibody (BD Biosciences) either directly linked to PE ("PE-protocol," direct immunofluorescence) or followed by incubation with fluorescein isothiocyanate (FITC)–conjugated goat anti–mouse secondary Ig (BD Biosciences; "FITC-protocol," indirect immunofluorescence). To test for specific binding of tTF-NGR versus tTF, we incubated HUVECs for 12 minutes at 37°C with His-tagged tTF-NGR or tTF at increasing concentrations. After washing of the cells, binding of tTF-NGR or tTF was verified using anti–His-Tag antibody (Novagen, Madison, WI) as described above. To show competition for binding sites, we preincubated HUVECs with excess amounts of tTF-NGR without His-Tag and then performed tTF-NGR binding studies as described above. To further characterize tTF-NGR (and deamidation product) binding sites, HUVECs were incubated with AB against either CD13, $\alpha_v\beta_3$ (CD51/CD61) or thrombomodulin (control) for 12 minutes at 37°C, followed by washing. Then the cells were either incubated without or with 150 μg/mL tTF-NGR or tTF for 24 minutes at 37°C. Subsequently, cells were washed and directly measured when AB were PE-linked ("PE-protocol"), or AB were detected by incubation with FITC-conjugated goat anti–mouse secondary Ig labeling ("FITC-protocol") as described above and then measured (FACSCalibur flow cytometer; Becton Dickinson, San Jose, CA).

Cell culture

HUVECs were from BD Biosciences. The human melanoma derived cell line M21 was kindly provided by Dr S. Silletti (University of California, San Diego, CA). The human fibrosarcoma cell line HT1080 and the human lung cancer cell line A549 (adenocarcinoma) were described elsewhere.[24-26] The M21 cell line was cultured in RPMI 1640 medium supplemented with 10% fetal calf serum (FCS; GIBCO-BRL, Eggenstein, Germany) and 2 mM L-glutamine (GIBCO-BRL). The HT1080 cell line was cultured in Dulbecco medium supplemented with 10% FCS, and the A549 cell line was cultured in HAM F12 medium (GIBCO-BRL) supplemented with 10% FCS and 2 mM L-glutamine.

Tumor mouse models

The tumor cells for the experiments were grown as attached monolayer cultures, dissociated in trypsin, centrifuged, and washed in phosphate-buffered saline (PBS) and resuspended in PBS. For evaluation of the antitumor effect and measuring the vascular volume fraction, 9- to 12-week-old male BALB/c/nude mice (Charles River, Sulzfeld, Germany) were injected subcutaneously with the M21, A549, or HT1080 cells in one rear flank with 2×10^6 cells/mouse in 100 μL. To estimate the volume of the skin tumor, the exposed surface of the tumor was measured in 2 perpendicular directions, and the volume was calculated as (length × width^2 × π/6). Tumor growth was allowed to a volume of approximately 30 to 300 mm^3 (A549) and 300 to 1700 mm^3 (M21, HT1080), respectively. Different tumor volumes were chosen as starting points for randomization and treatment to study possible tumor growth retarding effects of early and tumor shrinkage of late treatment onset. The mice were randomly assigned to different experimental groups. Group 1 received 0.9% NaCl (100 μL), group 2 tTF (30 μg/mouse in 100 μL 0.9% NaCl), and group 3 tTF-NGR (30 μg/mouse in 100 μL 0.9% NaCl) via intravenous tail vein injection. tTF and tTF-NGR were compared using identical μg-doses and not in equimolar concentrations, because the difference of molecular weight is low (2.2%). In additional experiments with the HT1080 model, saline or experimental drugs were also injected subcutaneously distant from the tumors using various schedules and doses. Depending on the growth kinetics of the single tumor models and the time of treatment onset, injections were repeated twice weekly no more than 7 times (slow growing A549) or up to daily no more than 5 times (M21, HT1080).

For subcutaneous therapy studies, we used CD-1 nude mice (Charles River). To study the development of resistance, mice with regrowing tumors after an observation period without tTF-NGR therapy were re-exposed to subcutaneous treatment with the compound, and control mice with tumors at similar size were treated for the first time in parallel.

Two days after the last injection, some mice were killed by cervical dislocation in deep CO_2 anesthesia, in agreement with standard regulations and the project license. Subsequently, the tumor was removed for histologic studies. For toxicity studies, tTF-NGR, tTF, and 0.9% NaCl solutions were injected in the tail vain. The mice were killed 60 minutes, 4 hours, or 24 hours after the injection, and the tumor and major organs were removed, fixed in formaldehyde, and paraffin embedded for histologic studies. According to our project license,

animals had to be killed when tumors became too large, if mice lost more than 20% of body weight, or at signs of pain. This limited the duration of observation in our experiments.

Parametric MRI

For measuring the vascular volume fraction (VVF) by contrast enhanced MRI, we based our procedure on a method described previously.[15] We divided the mice into 3 groups after the tumor had grown to a volume of approximately 1000 mm^3. The first group received a single dose of 30 μg tTF-NGR in 200 μL 0.9% NaCl solution, the second received the same amount of tTF solution, and the third group 200 μL 0.9% NaCl solution (saline) intravenously in the tail vein. Approximately 4 to 8 hours after the injection, MRI was performed on a clinical 1.5 Tesla whole body MR system (Interna; Philips Medical Systems, Best, The Netherlands) using a microscopy surface coil with a diameter of 47 mm (Philips Medical Systems). For measuring VVF, tumor bearing animals were anaesthetized by an intraperitoneal injection of ketamine (125 mg/kg body weight [bw]) and xylazine (12.5 mg/kg bw). To allow vascular access, the jugular vein was cannulated by a 2.5 French catheter (SIMS Portex, Kent, United Kingdom). To depict anatomical details, the tumors were imaged using a T2-weighted Turbo Spin Echo sequence. For measuring the perfused tumor volume (VVF), a fast spoiled gradient dual echo EPI sequence was acquired before and after intravenous injection of ultrasmall superparamagnetic iron oxide nanoparticles (USPIO; SHU 555 C; Schering AG, Berlin, Germany). SHU 555 C is currently situated in clinical phase III trials. The change in transverse relaxation rate (ΔR2*) was calculated, and VVF was determined by calibration of the ΔR2* of the tumor over ΔR2* of the muscle. Thereafter, the mice were killed, and the tumor was removed for histologic studies.

All procedures on animals were performed in accordance with German regulations (Tierversuchsgesetz § 8 Abs 2) and specifically approved in the form of a project license by the state review committee on animal care and experiments.

For patient measurements, a multi-echo relaxometry sequence was performed again on a clinical 1.5-Tesla whole-body MR scanner (Achieva; Philips Medical Systems). For anatomic orientation, transverse T2-weighted images were obtained. The change of the transverse relaxation rate (ΔR2*) was determined pre- and postinjection of the clinical approved superparamagnetic iron oxide (SPIO) SHU 555 A (Resovist; Schering AG). ΔR2* changes were determined in regions of interest (ROIs) at corresponding ΔR2*-maps, and the VVF was calculated. Ethical approval for this monitoring of treatment was obtained from the joint ethical board of the University of Muenster and the locoregional physician's chamber of Westfalen-Lippe. Informed consent was obtained in accordance with the Declaration of Helsinki.

Histology

Histologic analyses were performed on 4% paraformaldehyde fixed and paraffin-embedded tissues as described previously.[4] Briefly, tissues embedded in paraffin were cut to 4-μm sections and transferred onto glass slides. At least 10 sections per sample were available for evaluation. For identification of thrombosis, hematoxylin and eosin (H&E)–stained sections were examined using conventional light microscopy for signs of intratumoral thrombosis in a blinded fashion. Thrombosis of intratumoral vessels was defined according to the following criteria: total or incomplete occlusion by closely packed erythrocytes, blurring of the vessel outline, and the presence of aggregated platelets and fibrin deposition.

Statistical analysis

Statistical significance of differences was tested by the Mann-Whitney rank sum test for independent groups. Two-sided *P* values less than .05 were considered significant.

Results

Cloning, expression, and characterization of tTF/tTF-NGR

For targeting of tumor vasculature, we used an NGR-peptide that selectively bound to CD13 expressed on tumor vessels but not to CD13 expressed on normal tissue.[21] The NGR motif GNGRAHA was fused to tTF using a PCR assembly cloning strategy for expression in *E coli*. The fusion protein tTF-NGR consists of a $(His)_6$ sequence (histidin tag) to allow purification using immobilized metal-chelate affinity chromatography (IMAC), enterokinase- and thrombin-cleavage sites linked to the N-terminus of tTF, and the NGR peptide linked to the C-terminus of tTF.

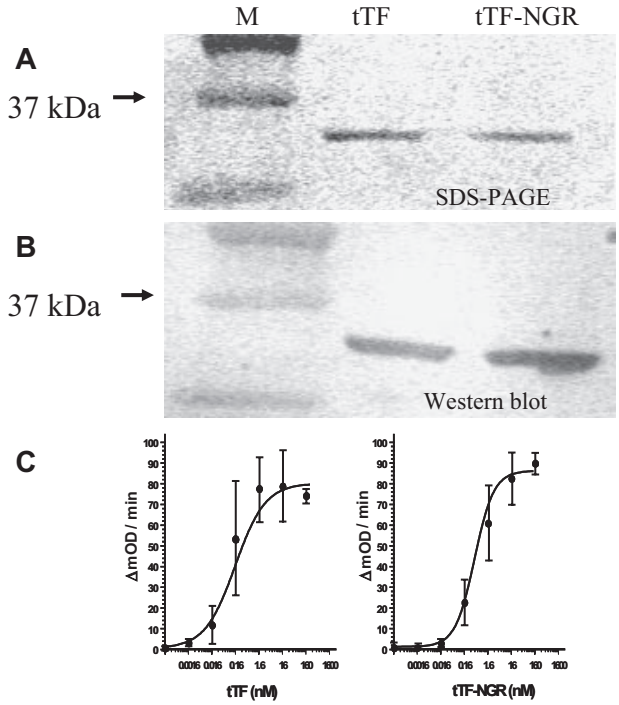

Figure 1. tTF/tTF-NGR characterization. (A,B) SDS-PAGE and Western blot analysis of tTF and tTF-NGR. (C) Ability of the fusion proteins to enhance the specific proteolytic activation of FX by FVIIa in the presence of phospholipids was evaluated by Michaelis-Menten analysis as described by Ruf et al.[22] The calculated Michaelis constants (K_m) of the hyperbolic parts of the kinetic curves were 0.2 nM (tTF) and 0.4 nM (tTF-NGR), respectively. Mean values of 3-fold assays are given with SD.

The fusion protein tTF-NGR and tTF were expressed at approximately 25 mg/L and were localized in inclusion bodies. The inclusion bodies could be solubilized in denaturing buffer and purified to approximately 95% purity. After refolding and dialyzing, we confirmed the identity of the protein by mass spectroscopy (data not shown), SDS-PAGE, and Western blot (Figure 1A,B).

Functional characterization of tTF and tTF-NGR

The ability of tTF and tTF-NGR to enhance the specific proteolytic activation of FX by FVIIa was demonstrated by Michaelis-Menten analyses (for representative experiment see Figure 1C). The calculated Michaelis constants (K_m) for tTF and tTF-NGR were within the range reported in the literature.[23] This demonstrates that the ligation of the peptide sequence to the C-terminus of tTF did not significantly affect its functional activity.

Binding studies

To study specific binding of tTF-NGR (and deamidation product) with flow cytometry, we first characterized HUVECs as carrying relevant (CD13, $\alpha_v\beta_3$) and control (thrombomodulin) binding sites (Figure 2A). Next, we found specific binding of His-tagged tTF-NGR, but not tTF, which could be inhibited by tTF-NGR without His-tag (Figure 2 B gated events). There was also a small percentage of nonspecific binding of both tTF and tTF-NGR to the cells, which could not be inhibited (Figure 2B left of gate). Next, we showed replacement of anti-CD13 and

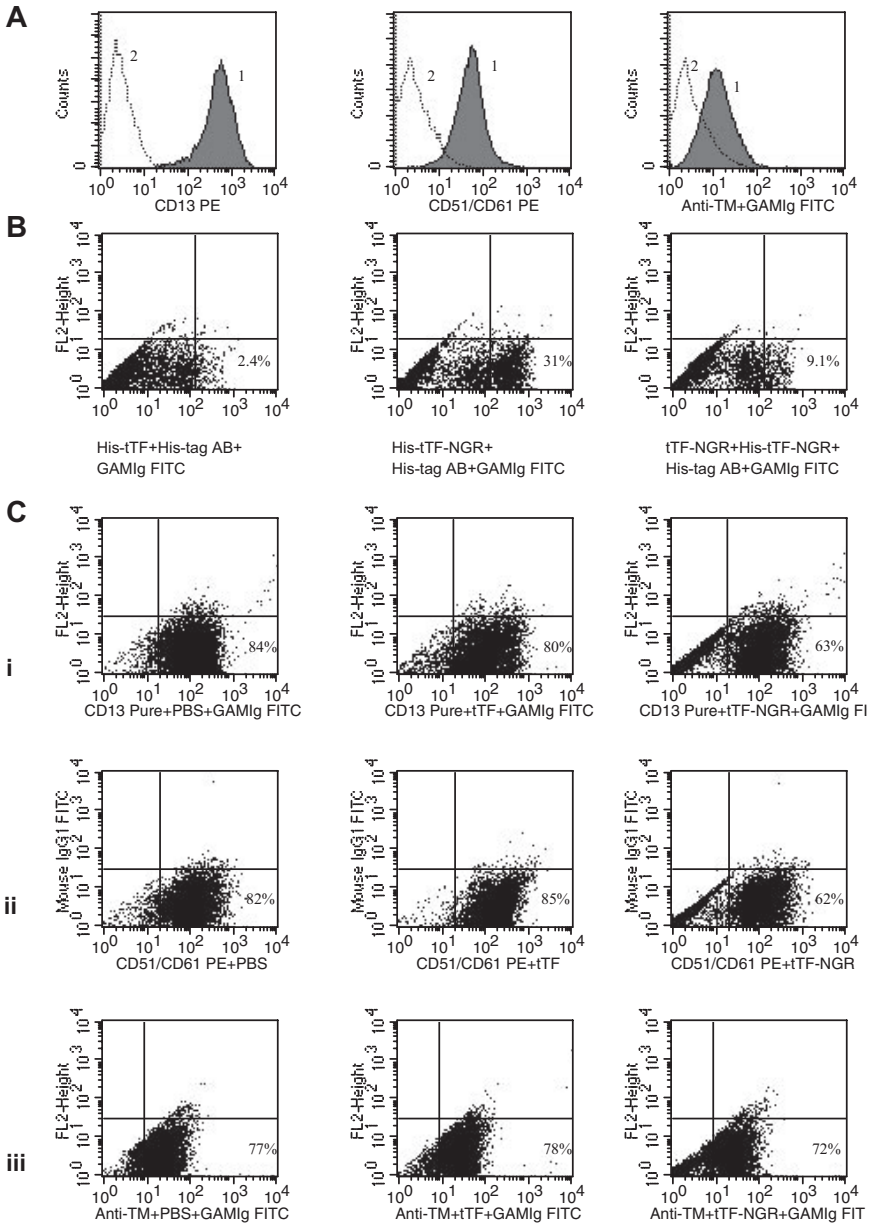

Figure 2. Binding studies by flow cytometry. (A) Presence of CD13 (left panel), $\alpha_v\beta_3$/CD51/CD61 (center), and thrombomodulin (right) on HUVECs as shown by specific AB (curve 1). Curve 2, isotype control. (B) Lack of binding of His-tagged tTF (without NGR) as shown with anti–His-AB (left dot plot). Binding of His-tagged tTF-NGR as shown with anti–His-tag-AB (center). Inhibition of binding of His-tagged tTF-NGR by double amounts of tTF-NGR without His-tag (right). We used single color fluorescence detecting cell-bound His-tagged tTF (left) or His-tagged tTF-NGR (center; step 1) by visualizing with His-tag mouse monoclonal AB (step 2) and then with FITC-labeled goat anti–mouse Ig (step 3). In the right dot plot, cells were first incubated with tTF-NGR without His-tag and were then incubated with His-tagged tTF-NGR (see step 1 above) with the identical visualization sequence as above (see steps 2 and 3). (C) Binding of AB to CD13 (i left), $\alpha_v\beta_3$ (ii left) binding sites and thrombomodulin control site (iii left). Replacement of AB-binding by 150 μg/mL tTF-NGR to CD13 (i, right), $\alpha_v\beta_3$ (ii right) in contrast to tTF (i,ii center). No competition of 150 μg/mL tTF-NGR with AB-binding to thrombomodulin (iii right). Dot plots with single color show fluorescence intensity on x-axis. The y-axis titled "FL2-Height" was not occupied in all dot plots using the "FITC-protocol" (see "Methods") and the y-axis (FL-1) using the "PE-protocol" (see "Methods") was occupied with mouse IgG 1 FITC to yield a better visualization of the cell populations.

anti-$\alpha_v\beta_3$ AB from their respective binding sites by excess amounts of tTF-NGR in contrast to tTF (Figure 2C). Approximately 20% of the AB-binding to CD13 and to $\alpha_v\beta_3$ could be replaced by tTF-NGR, in contrast to tTF. There was no replacement by tTF-NGR of AB binding to control targets such as thrombomodulin (Figure 2C).

Effect of tTF-NGR on growth of xenotransplanted tumors in mice

Next, we determined the antitumor activity of tTF-NGR in BALB/c nude mice bearing 30- to 100-mm^3 A549 tumors. Because of the slower tumor growth, the drug and the controls were administered 7 times at intervals of 3 to 4 days. The pooled results of 2 independent experiments are presented in Figure 3A. After 4 and 5 injections of tTF-NGR, a significant growth inhibition of the A549 tumors was observed (in comparison to the saline and tTF group, respectively; $P = .008$ and $P = .007$, respectively).

The antitumor activity of tTF-NGR was further determined in a series of experiments using BALB/c nude mice bearing 300- to 1000-mm^3 M21 tumors. The controls and tTF-NGR solutions were administered intravenously 5 times at intervals of 24 hours. The pooled results of 2 independent experiments are presented in Figure 3B. The tumor growth was significantly inhibited by day 4 of the treatment ($P = .016$) in comparison to saline treatment, and by day 5 of the treatment in comparison to tTF treatment ($P = .035$).

Subsequently, the antitumor activity of tTF-NGR was determined in BALB/c nude mice bearing HT1080 tumors. The controls and tTF-NGR were administered intravenously 3 times at intervals of 24 hours. The pooled results of 2 independent experiments are presented in Figure 3C. The tumor growth was significantly inhibited by day 7 of the treatment ($P = .023$) in comparison to saline treatment and by day 7 of the treatment in comparison to tTF treatment ($P = .02$).

Alternative routes of application and re-exposition experiments

Because repeated intravenous injections caused necrosis of tail tips in the injected animals, and to facilitate potential clinical use, we studied alternative routes of application. Subcutaneous injections

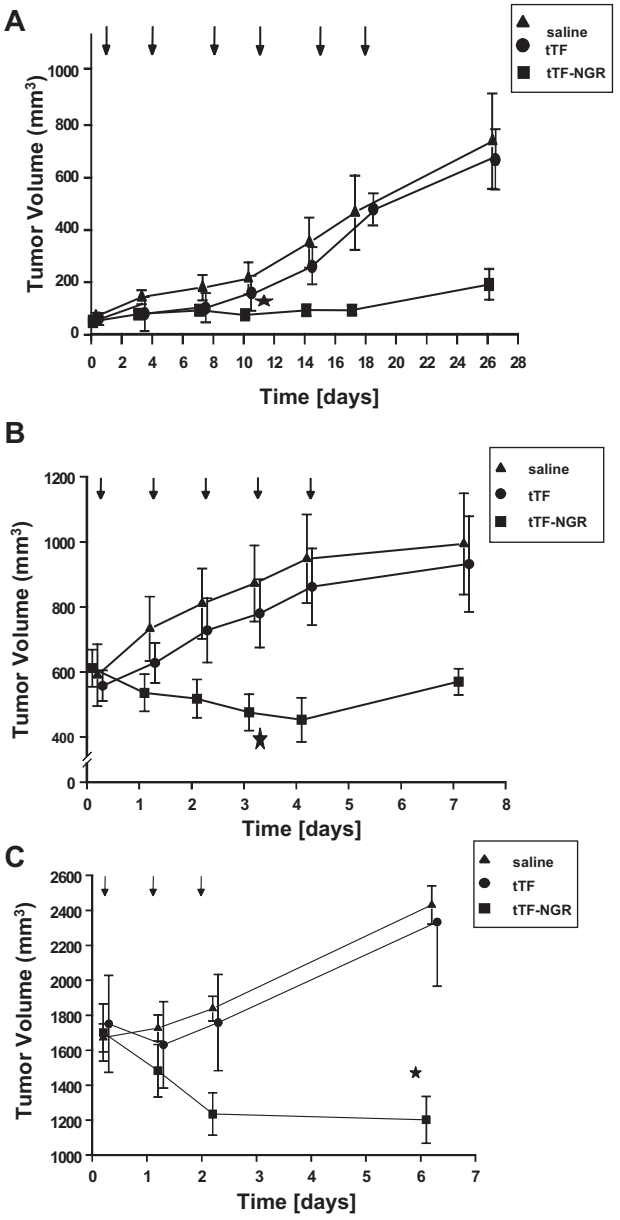

Figure 3. Tumor inhibition. (A) Growth inhibition of human lung cancer (A549) transplanted into athymic nude mice by intravenous administration of tTF-NGR (n = 11) compared with the administration of tTF (n = 4) or saline (0.9% NaCl, n = 10). Arrows indicate the time points of injection. Data are presented as means ± SE. The tumor growth was significantly retarded by tTF-NGR after the fourth injection in comparison to the saline group ($P = .008$, Mann-Whitney test) and after the fifth tTF-NGR injection in comparison to the tTF group ($P = .007$, Mann-Whitney test). * denotes first day of statistical significance between tTF-NGR and saline. (B) Effect of tTF-NGR on the growth of melanoma xenotransplants in mice. Growth inhibition of human melanoma (M21) transplanted into athymic nude mice by intravenous administration of tTF-NGR (n = 7) compared with the administration of tTF (n = 11) or saline (0.9% NaCl, n = 9). Time (days) shown represent days after first treatment. Arrows indicate the time point of injection. Data are presented as means ± SE. The tumor growth was significantly retarded on day 4 of the tTF-NGR treatment in comparison to the saline group ($P = .016$, Mann-Whitney test) and on day 5 in comparison to the tTF group ($P = .035$, Mann-Whitney test). * denotes first day of statistical significance between tTF-NGR and saline. (C) Effect of tTF-NGR on the growth of fibrosarcoma xenotransplants in mice. Growth inhibition of human fibrosarcoma (HT1080) transplanted into athymic nude mice by intravenous administration of tTF-NGR (n = 8) compared with the administration of tTF (n = 14) or saline (0.9% NaCl, n = 15). Time (days) shown represent days after first treatment. Arrows indicate the time point of injection. Data are presented as means ± SE. The tumor growth was significantly retarded at day 6 of the tTF-NGR treatment in comparison to the saline group ($P = .023$, Mann-Whitney test) and at day 6 in comparison to the tTF group ($P = .02$, Mann-Whitney test). * denotes statistical significance between tTF-NGR and saline.

of 1, 3, or 5 mg/kg tTF-NGR either delayed (Figure 4A) HT1080 tumor growth or induced tumor shrinkage and subsequent growth delay (Figure 4B) compared with saline controls. Furthermore, using higher and toxic doses we could observe small numbers of complete remissions (CR) with no regrowth even after prolonged observation (Figure 4B). To study development of resistance, in some experiments, mice with regrowing tumors after an observation period without tTF-NGR therapy (> 3 weeks) were re-exposed to subcutaneous treatment with the compound, and control mice with tumors at similar size were treated for the first time in parallel. Results showed lack of resistance development upon re-exposition to tTF-NGR, because HT1080 tumor shrinkage was similar comparing the effects of first versus second treatment applications (Figure 4C).

Infarction of M21 tumors in mice

To test whether tTF-NGR was able to promote thrombosis in tumor vasculature, we treated BALB/c nude mice bearing a M21 tumor of 600 mm^3 with 2 mg/kg body weight tTF-NGR and 0.9% NaCl solution as a control. In the tTF-NGR–treated mice, the tumor was bruised and blackened, indicating blood pooling due to vascular disruption after the injection of tTF-NGR (Figure 5A). After 60 minutes, the tumor was completely removed for histologic studies. Figure 5B shows areas of hemorrhage in the tumor of the mouse treated with tTF-NGR in contrast to the vital appearance of the tumor treated with saline (Figure 5C). Microscopic studies revealed that tumor vessels of the malignant melanoma treated with tTF-NGR were thrombosed (Figure 6A,B) in contrast to the tumor vessels of the saline-treated (Figure 6C,D) or the tTF-treated (Figure 6E,F) animals. Thus, the presumable mode of action of tTF-NGR (ie, the thrombotic occlusion of tumor vessels) was confirmed by these observations.

Selectivity and tolerability

The high selectivity of vascular occlusion by tTF-NGR for tumor blood vessels was demonstrated by the fact that no visible thrombosis occurred in the vasculature of normal tissues such as heart, kidney, liver, and lung at therapeutic intravenous doses (Figure 5D-G). In general, toxicity of tTF-NGR at therapeutic dose levels was low. We observed tail tip necrosis after repeated intravenous and intracutaneous bleeding after subcutaneous injections. There were occasional deaths in all groups of mice during experiments, occurring without clear dose-relation. However, dose escalation (3-9 mg/kg) done in the subcutaneous therapy series revealed increasing toxicity with greater than 10% death during the observation period. Thus, superiority of the subcutaneous over the intravenous route for therapeutic range could not be shown. Dose escalation of single intravenous injections in non–tumor-bearing mice revealed intravenous LD_{10} (lethal dose for 10% of the animals) as being greater than or equal to 5 mg/kg. At these doses, some of the animals showed pulmonary embolism in postmortem histology (details not shown).

Parametric MRI in mice tumor xenografts

To obtain further evidence for the therapeutic principle of tTF-NGR, we administered a single dose of either tTF-NGR, tTF, or saline to HT1080 bearing BALB/c nude mice. After 4 to 8 hours, we measured the VVF by USPIO-enhanced MRI. The VVF was significantly reduced in the tTF-NGR treated group compared with the saline group ($P < .005$; Figure 7). tTF alone had only minor effects on VVF compared with saline control (Figure 7). Moreover,

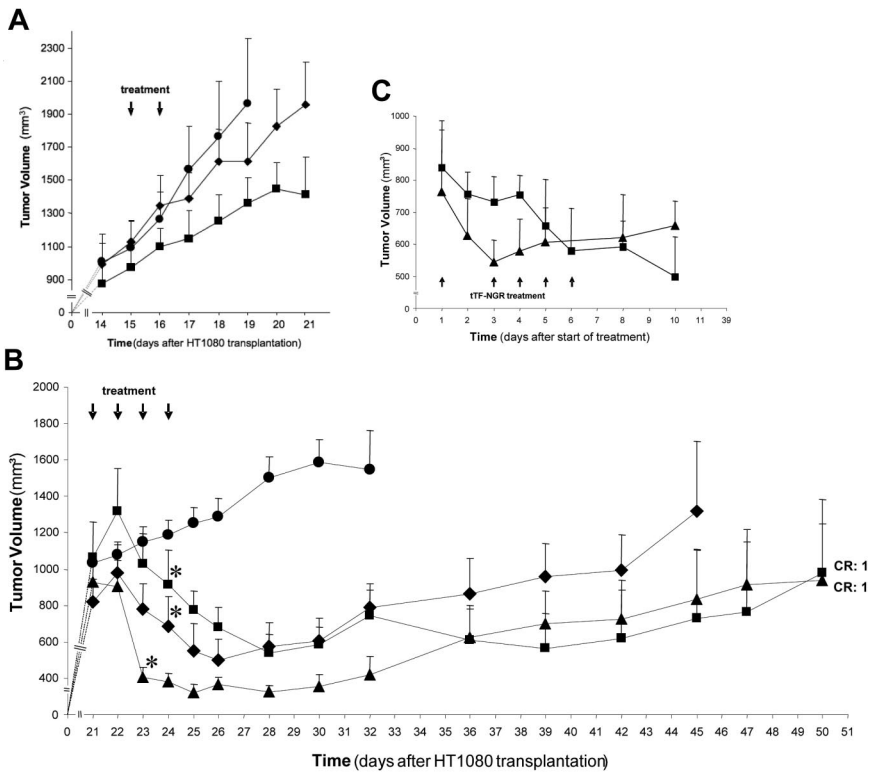

Figure 4. Long-term effect of intravenous and subcutaneous application of tTF-NGR on the growth of fibrosarcoma (HT1080) xenotransplants in mice. (A) Growth inhibition of HT1080 by subcutaneous administration of tTF-NGR (1 mg/kg bw [◆], n = 7, or 3 mg/kg bw [■], n = 7, respectively) compared with saline ([●], n = 6). Arrows indicate the time points of injection (2 applications). Data are presented as means ± SE. (B) Tumor shrinkage and growth inhibition of HT1080 by subcutaneous administration of tTF-NGR (3 mg/kg bw [■], n = 7, or 5 mg/kg bw [▲], n = 7, respectively) compared with the intravenous administration of tTF-NGR (1 mg/kg bw [◆], n = 6) or saline ([●], n = 7). Arrows indicate the time points of injection (4 applications). Data are presented as means with SE. * denotes first day of statistical significance between tTF-NGR and saline (Mann-Whitney rank-sum test for independent groups; $P < .05$ were considered significant). At day 32, the control cohort was removed because of tumor size or spontaneous ulceration. CR, complete remission. (C) Re-exposition of prior tTF-NGR–treated (after regrowth, ▲) in comparison to previously untreated tumor-bearing animals (■). Growth of HT1080 was inhibited by subcutaneous administration of tTF-NGR (3 mg/kg bw, each group with n = 4). Arrows indicate the time points of injection. Data are presented as means ± SE. There were no significant differences between both groups.

as demonstrated by histology, the tTF-NGR–treated tumors showed gross infarction of the tumor tissue (Figure 7).

Clinical cases

For clinical, first-in-man application, tTF-NGR was administered to terminal stage cancer patients who had progressive disease after several lines of standard therapy. Treatment was performed upon written informed consent of the patients and with approval of the joint ethical board of the University of Muenster and the locoregional physician's chamber of Westfalen-Lippe in accordance with German law. tTF-NGR was solved in saline and given as a 1-hour intravenous infusion via a central venous access, starting at 1 mg/m^2 body surface area and allowing for repeated dosing after 1 week. This starting dose was well below 10% of the LD_{10} determined in mouse toxicity studies.

The first patient treated was a 56-year-old woman suffering from an advanced cholangiocarcinoma including malignant ascites with progression upon palliative therapy with gemcitabine and anthracyclines. The patient obtained 1, 1.5, and 2 mg/m^2 doses of tTF-NGR at weekly intervals. Tolerability of tTF-NGR under clinical and cardiopulmonary monitoring was without side effects. However, directly after infusion of the first dose, there was a decrease in the platelet count from $129 \times 10^3/\mu L$ to $90 \times 10^3/\mu L$, a decrease of alpha-2-antiplasmin (from 80% to 64%), and antithrombin levels (from 55% to 49%). In addition, we observed a slight increase of the prothrombin time (from 14.6 to 16.2 seconds). These changes were repeatedly observed under the following infusions, but reversible after 24 hours. In this patient, a well vascularized tumor lesion of the liver was monitored by parametric MRI before and after tTF-NGR application. The lesion showed a maximum reduction of the vascular volume fraction (VVF) of 24.9% approximately 5 hours after the first tTF-NGR application, while the majority of the liver lesions, which seemed widely necrotic in anatomic T2-weighted images, revealed no measurable changes (Figure 8). After 3 applications, however, therapy was stopped because of disease progression.

The second patient presented was a 28-year-old woman suffering from metastatic adenocarcinoma of the lung with disease progression after 4 lines of chemotherapy including bevacizumab and palliative radiation. The patient obtained a 3.0 mg/m^2 dose of tTF-NGR and a breast metastasis with low vascularization, monitored by parametric MRI, showed an approximately 18% reduction in VVF (Figure 8) with a decrease in platelet count from $198 \times 10^3/\mu L$ to $162 \times 10^3/\mu L$, decrease in alpha-2-antiplasmin (from 93% to 87%), and decrease in antithrombin levels (from 62% to 56%). There were no side effects, but disease progression.

tTF-NGR was given to 3 additional patients with late-stage disease (mesothelioma, multiple myeloma with extramedullar tumor formation, metastatic germ cell tumor) progressive after several lines of standard therapy in doses up to 4.0 mg/m^2. One of those (mesothelioma) showed reduction of VVF in tumor ROIs in contrast to normal tissue, and good tolerability was observed in all of the patients.

Discussion

There are only a few reports on cancer therapy by antibody-directed targeting of human TF to tumor vasculature showing some growth reduction and tumor shrinkage.[10-12] One major limitation of using antibodies for targeting of tTF is that the large antibody molecule may have difficulties penetrating the tumor where the blood supply is inadequate.[27,28] Another major problem is the nonspecific uptake of the antibody by the reticuloendothelial system of organs such as liver, spleen, and bone marrow. Therefore, the dose-limiting toxicities of radiolabeled or toxin-conjugated antibodies are liver or bone marrow toxicities.[29,30] To prevent the

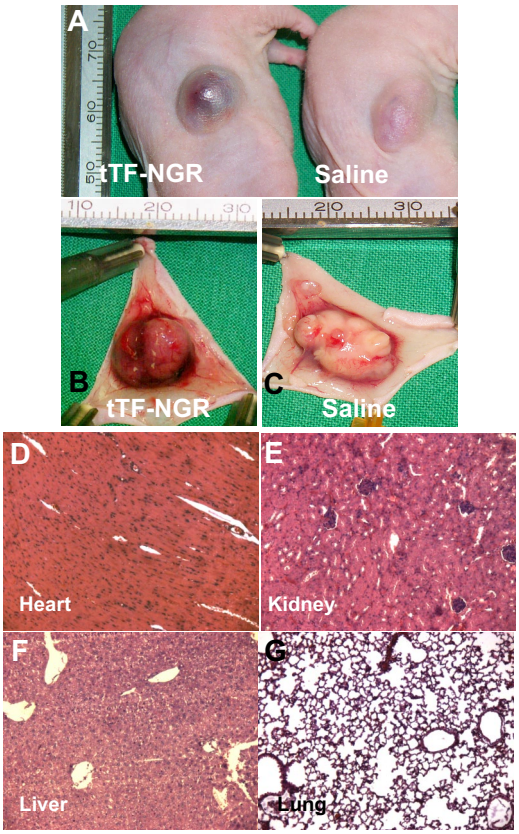

Figure 5. Representative photographs of the malignant melanoma-bearing mice and H&E staining of normal tissue of the tTF-NGR–treated mice. (A) Mice are shown 20 minutes after injection of tTF-NGR (left) and saline (right). The tumor treated with tTF-NGR was bruised and blackened, indicating blood pooling due to vascular disruption. (B) The resected tumor treated with tTF-NGR exhibited areas of hemorrhage in contrast to the vital appearance of the tumor treated with saline (C). Heart (D), kidney (E), liver (F), and lung (G) of the tTF-NGR–treated tumor-bearing mice showed no visible thrombosis. Original magnification, ×200.

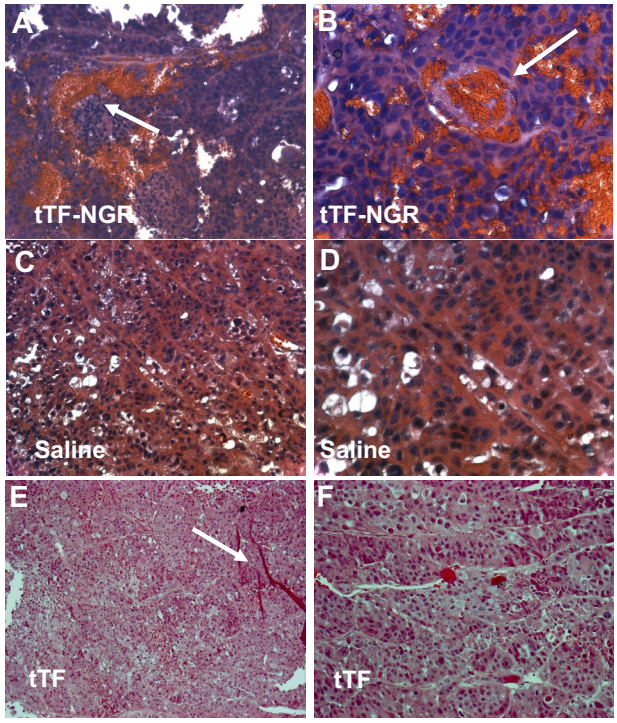

Figure 6. H&E staining of human xenotransplants (M21) in mice. H&E staining of the tTF-NGR–treated tumors showed thrombosis of blood vessels and extensive blood pooling due to vascular disruption (arrows indicating the occluded blood vessels; A,B). The tumors in the saline (C,D) or the tTF (E,F)–treated control group exhibited no thrombosis. Red stripes in panel E are artifacts (arrow). Original magnifications, ×200 (A,C,E) and ×400 (B,D,F).

drawbacks of this approach, we expressed a fusion protein consisting of tTF and a small peptide coupled to the C-terminus of tTF. Based on the known crystal structure of the tTF:VIIa complex,[31] the fusion of the small GNGRAHA peptide would allow the generated tTF-peptide fusion protein to adopt an orientation perpendicular to the phospholipid membrane of the endothelial cell similar to native TF. On the other hand, ligation of the peptide to the C-terminus of tTF should not result in steric hinderance of the interaction of tTF with FVIIa and its substrate FX. Peptides are much smaller than antibodies, and they usually do not bind to the reticuloendothelial system and show no antigenicity. In addition, they are chemically stable and relatively easy to derivatize (eg, cyclic NGR analogs, tTF fragments).[32]

For targeting tTF to the tumor endothelium, we chose an NGR motif, which was discovered by in vivo screening of phage libraries.[33] Later, aminopeptidase N (CD13) was identified as binding site for the NGR motif, which is up-regulated within mouse and human tumors.[21,34,35] CD13 is up-regulated in response to hypoxia and angiogenic growth factors, and it plays a role in the control of endothelial cell morphogenesis, and inhibition of the CD13 pathway abrogates endothelial cell migration, invasion, and morphogenesis.[18,35] Besides its expression on endothelial cells, CD13 is expressed on hematopoietic cells and epithelial cells of the proximal tubules in the normal kidney.[21,36] Interestingly, tumor-targeting properties of NGR-drug conjugates relies partially on recognition of CD13 isoforms selectively expressed within tumor-associated vessels but not on normal tissues.[21] Furthermore, NGR can rapidly convert to isoaspartate-glycine-arginine (*iso*DGR) by asparagine deamidation, generating $\alpha_v\beta_3$ ligands.[22] This adds further advantage to the binding properties of tTF-NGR targeting 2 sites preferentially expressed or up-regulated on tumor endothelial cells.

The NGR-containing oligopeptide did not significantly alter the cofactor activity of tTF as measured in a FX activation assay. The hypothesized mechanism of in vivo inhibition of tumor growth by thrombosis in the tumor vasculature was proven in 3 tumor models in mice. Application of tTF-NGR to mice xenotransplanted with the slow growing human adenocarcinoma A549 resulted in significant growth retardation. In the more aggressive tumor model of human melanoma M21, administration of tTF-NGR resulted in significant regression of tumor size. However, complete remissions, as reported by Nilsson et al,[10] using a fusion protein of a single chain antibody directed against the ED-B domain of fibronectin with tTF, was only observed sporadically after subcutaneous treatment with higher and toxic doses in the HT1080 fibrosarcoma. This might be due to the lower affinity of NGR toward its target compared with an antibody fragment as used in the previous report.

Tumor histology demonstrated thrombotic occlusion in up to 90% of the tumor vessels in the tTF-NGR–treated mice. The fact that tTF fused to the NGR-target moiety, but not untargeted tTF, induced thrombosis with decreased VVF as shown by contrast enhanced MRI studies and subsequent tumor shrinkage or growth delay supports the hypothesis that by binding of tTF-NGR to the cell surface of tumor endothelium, tTF recovers, in part, its native function. Furthermore, the specificity of our approach of targeting CD13 and $\alpha_v\beta_3$ on tumor endothelium is underlined by the

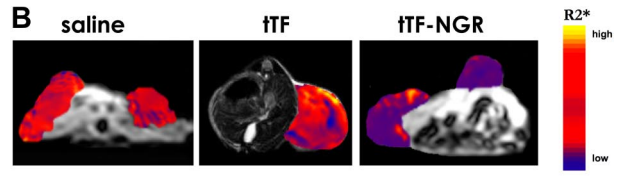

	dR2* [ms-1]	VVF [%]
saline	0.0202	1.69
tTF	0.0149	1.46
tTF-NGR	0.0097	0.53

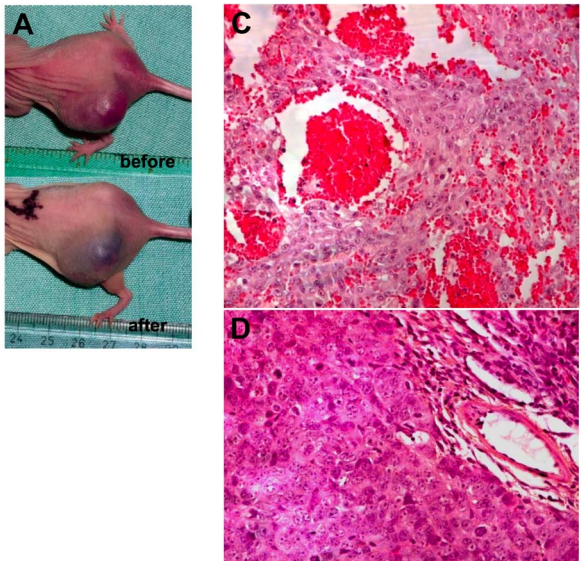

Figure 7. Fibrosarcoma-bearing mouse before and after injection of tTF-NGR. (A) Photograph of a fibrosarcoma-bearing mouse before and after injection of tTF-NGR (1.5 mg/kg body weight). The tumor was blackened after tTF-NGR injection, indicating blood pooling due to vascular disruption. (B) Measurement of the vascular volume fraction (VVF) by contrast enhanced MRI. By measuring the VVF, a significantly reduced blood volume in the tTF-NGR–treated mouse was detected compared with saline controls, whereas non-targeted tTF had only minor effects. The change in the transverse relaxation rate (ΔR2*), as displayed in the color coded overlay, was significantly reduced after treatment with tTF-NGR. (C) H&E staining of the tTF-NGR–treated tumor showed thrombosis in blood vessels, blood pooling, and vascular disruption. (D) The tumor in the saline-treated mouse exhibited no thrombosis.

observation of no visible thrombosis or cell damage in liver, kidney, heart, or lung. It is unlikely that the antitumor effect of tTF-NGR is solely due to its NGR target moiety because administration of NGR sequences containing peptides alone displayed no antitumor activity in a previous study.[21]

The phenomenon of tumor regrowth after the end of treatment observed here has been also described by other groups using tTF-based antivascular treatment.[10,11] However, regrowth of residual tumor cells might be overcome by other schedules and doses. Combinations with cytotoxic drugs[14] or radiation therapy might further enhance the antitumor efficacy of tTF-NGR (see below). Besides these modifications, a further therapeutic benefit could be achieved using cyclic NGR-peptides coupled to tTF because of the higher affinity of the cyclic NGR-peptides to CD13, thus increasing the numbers of tTF molecules bound to the tumor endothelium.[37]

So far, there are only limited studies on toxicity. By histologic analysis after intravenous administration of tTF-NGR at therapeutic doses, neither areas of hemorrhage and thrombosis nor other abnormalities were detected in normal organs. The selectivity for thrombosis in tumor vessels is most likely due to the specific binding of tTF-NGR to CD13[21] and $\alpha_v\beta_3$[15] on tumor endothelium.

The lack of a thrombotic effect of tTF-NGR in the vasculature of heart, lung, kidney, and liver may be additionally explained by differential expression of phosphatidylserine (PS) on tumor endothelium compared with normal endothelium. PS expression on the cell surface is essential for coagulation because it enables the binding of coagulation factors such as FVIIa and FX, thus coordinating the assembly of the coagulation initiation complexes.[38-40] Normal tissues segregate PS to the inner surface of the plasma membrane phospholipid bilayer where it is unable to participate in thrombotic reactions. In contrast, tumor endothelial cells translocate PS to the external surface of the plasma membrane, thus supporting coagulation activation by tTF bound to tumor endothelium.[11] Such a supporting PS milieu might even be enhanced by inducing apoptosis through radiation or chemotherapy in conjunction with tTF-NGR. Homing of the NGR motif to tumor endothelium has been shown for breast carcinoma, melanoma, and Kaposi sarcoma.[8,16] In addition, we could demonstrate antitumor activity of tTF-NGR against a lung carcinoma and fibrosarcoma,

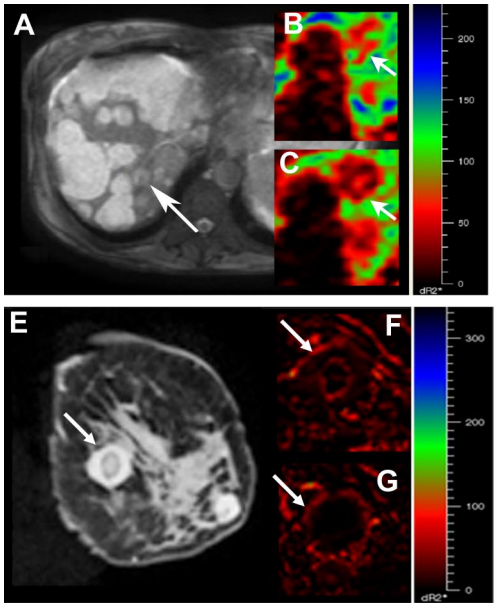

Figure 8. Patient MRIs. Top panel: MRI of a 56-year-old woman with an advanced cholangiocarcinoma. (A) The majority of the liver lesions revealed mainly necrotic and bright at the anatomic T2w image, whereas some smaller vascularized lesions exposed gray (arrow). Parametric, SPIO enhanced ΔR2*-maps of a well vascularized liver lesion (arrow) showed in correlation of pre- (B) to post- (C) tTF-NGR application a clear reduction of the vascular volume fraction (VVF). (D) The corresponding quantitative ΔR2* values revealed after repetitive measurements a 24.9% reduction of the mean tumor blood volume after tTF-NGR application, while the error bars describe the heterogeneous tumor blood volume pattern at the different localizations measured within the whole vascularized liver lesion. Bottom panel: MRI of a 28-year-old woman with lung adenocarcinoma (E). Breast metastasis (arrow) with low vascularization (possibly due to previous bevacizumab) before (F) and after (G) tTF-NGR application showing a reduction of the mean tumor blood volume of 18.2% (H). For details see top panel.

implying that NGR-mediated targeting of tumor vessels is a universally applicable approach in various cancers.

In summary, we have shown that tTF-NGR is an effective antitumor molecule in human tumor xenograft models by mediation of thrombosis in tumor vasculature. This first-in-man experience with very low doses of systemic tTF-NGR has shown that tumor perfusion can be selectively inhibited. This was demonstrated by the appropriate surrogate parameter (ie, VVF) for the putative mode of action in 3 of 5 patients treated so far without side effects. Thus, clinical trials with this new anticancer treatment approach are warranted to evaluate efficacy and safety in cancer patients.

Acknowledgments

This study was supported by grants from the Deutsche Forschungsgemeinschaft (Me 950/3-2), the Innovative Medizinische Forschung program of the Medical Faculty at the University of Muenster (ME 129822), and the Sybille-Hahne-Stiftung. J.D. contributed experiments that were performed to fulfill requirements for the MD degree.

Authorship

Contribution: R.B. performed research, analyzed data, and wrote the manuscript; T.K., C.S., T. Padro, T. Persigehl, J.D., and A.K. performed research and analyzed data; C.B. designed research and analyzed data; W.H. designed research; and R.M.M. and W.E.B. designed research, analyzed data, and wrote the manuscript.

Conflict-of-interest disclosure: W.E.B. and R.M.M. share a patent application on vascular targeting with TF-constructs. The other authors declare no competing financial interests.

Correspondence: Wolfgang E. Berdel, MD, Department of Medicine/Hematology and Oncology, University of Muenster, Albert-Schweitzer-Strasse 33, D-48129 Muenster, Germany; e-mail: berdel@uni-muenster.de.

References

1. Folkman J. Angiogenesis in cancer, vascular, rheumatoid, and other disease. Nat Med. 1995;1:27-31.
2. Carmeliet P. Mechanisms of angiogenesis and arteriogenesis. Nat Med. 2000;6:389-395.
3. Bieker R, Padro T, Kramer J, et al. Overexpression of basic fibroblast growth factor and autocrine stimulation in acute myeloid leukemia. Cancer Res. 2003;63:7241-7246.
4. Padro T, Ruiz S, Bieker R, et al. Increased angiogenesis in the bone marrow of patients with acute myeloid leukemia. Blood. 2000;95:2637-2644.
5. Hanahan D, Folkman J. Patterns and emerging mechanisms of the angiogenic switch during tumorigenesis. Cell. 1996;86:353-364.
6. Folkman J, Watson K, Ingber D, Hanahan D. Induction of angiogenesis during the transition from hyperplasia to neoplasia. Nature. 1989;339:58-61.
7. Ferrara N, Alitalo K. Clinical applications of angiogenic growth factors and their inhibitors. Nat Med. 1999;5:1359-1364.
8. Arap W, Pasqualini R, Ruoslahti E. Cancer treatment by targeted drug delivery to tumor vasculature in a mouse model. Science. 1998;279:377-380.
9. O'Reilly MS, Pirie-Shepherd S, Lane WS, Folkman J. Antiangiogenic activity of the cleaved conformation of the serpin antithrombin. Science. 1999;285:1926-1928.
10. Nilsson F, Kosmehl H, Zardi L, Neri D. Targeted delivery of tissue factor to the ED-B domain of fibronectin, a marker of angiogenesis, mediates the infarction of solid tumors in mice. Cancer Res. 2001;61:711-716.
11. Ran S, Gao B, Duffy S, Watkins L, Rote N, Thorpe PE. Infarction of solid Hodgkin's tumors in mice by antibody-directed targeting of tissue factor to tumor vasculature. Cancer Res. 1998;58:4646-4653.
12. Huang X, Molema G, King S, Watkins L, Edgington TS, Thorpe PE. Tumor infarction in mice by antibody-directed targeting of tissue factor to tumor vasculature. Science. 1997;275:547-550.
13. Morrissey JH, Macik BG, Neuenschwander PF, Comp PC. Quantitation of activated factor VII levels in plasma using a tissue factor mutant selectively deficient in promoting factor VII activation. Blood. 1993;81:734-744.
14. Liu C, Huang H, Donate F, et al. Prostate-specific membrane antigen directed selective thrombotic infarction of tumors. Cancer Res. 2002;62:5470-5475.
15. Kessler T, Bieker R, Padro T, et al. Inhibition of tumor growth by RGD peptide-directed delivery of truncated tissue factor to the tumor vasculature. Clin Cancer Res. 2005;11:6317-6324.
16. Pasqualini R, Koivunen E, Kain R, et al. Aminopeptidase N is a receptor for tumor-homing peptides and a target for inhibiting angiogenesis. Cancer Res. 2000;60:722-727.
17. Pasqualini R, Koivunen E, Ruoslahti E. A peptide isolated from phage display libraries is a structural and functional mimic of an RGD-binding site on integrins. J Cell Biol. 1995;130:1189-1196.
18. Bhagwat SV, Lahdenranta J, Giordano R, Arap W, Pasqualini R, Shapiro LH. CD13/APN is activated by angiogenic signals and is essential for capillary tube formation. Blood. 2001;97:652-659.
19. Drexler HG. Classification of acute myeloid leukemias–a comparison of FAB and immunophenotyping. Leukemia. 1987;1:697-705.
20. Riemann D, Kehlen A, Langner J. CD13–not just a marker in leukemia typing. Immunol Today. 1999;20:83-88.
21. Curnis F, Arrigoni G, Sacchi A, et al. Differential binding of drugs containing the NGR motif to CD13 isoforms in tumor vessels, epithelia, and myeloid cells. Cancer Res. 2002;62:867-874.
22. Corti A, Curnis F, Arap W, Pasqualini R. The neovasculature homing motif NGR: more than meets the eye. Blood. 2008;112:2628-2635.
23. Ruf W, Rehemtulla A, Morrissey JH, Edgington TS. Phospholipid-independent and-dependent interactions required for tissue factor receptor and cofactor function. J Biol Chem. 1991;266:2158-2166.
24. Topp MS, Koenigsmann M, Mire-Sluis A, et al. Recombinant human interleukin-4 inhibits growth of some human lung tumor cell lines in vitro and in vivo. Blood. 1993;82:2837-2844.
25. Topp MS, Papadimitriou CA, Eitelbach F, et al. Recombinant human interleukin 4 has antiproliferative activity on human tumor cell lines derived from epithelial and nonepithelial histologies. Cancer Res. 1995;55:2173-2176.
26. Rasheed S, Nelson-Rees WA, Toth EM, Arnstein P, Gardner MB. Characterization of a newly derived human sarcoma cell line (HT-1080). Cancer. 1974;33:1027-1033.
27. Vose JM. Immunotherapy for non-Hodgkin's lymphoma. Oncology (Williston Park). 2001;15:141-155.
28. Jain RK. Delivery of molecular and cellular medicine to solid tumors. Adv Drug Deliv Rev. 1997;26:71-90.
29. Neumeister P, Eibl M, Zinke-Cerwenka W, Scarpatetti M, Sill H, Linkesch W. Hepatic veno-occlusive disease in two patients with relapsed acute myeloid leukemia treated with anti-CD33 calicheamicin (CMA-676) immunoconjugate. Ann Hematol. 2001;80:119-120.
30. Thomas GE, Esteban JM, Raubitschek A, Wong JY. γ-Interferon administration after 90yttrium radiolabeled antibody therapy: survival and hematopoietic toxicity studies. Int J Radiat Oncol Biol Phys. 1995;31:529-534.
31. Banner DW, D'Arcy A, Chene C, et al. The crystal structure of the complex of blood coagulation factor VIIa with soluble tissue factor. Nature. 1996;380:41-46.
32. Aina OH, Sroka TC, Chen ML, Lam KS. Therapeutic cancer targeting peptides. Biopolymers. 2002;66:184-199.
33. Koivunen E, Wang B, Ruoslahti E. Phage libraries displaying cyclic peptides with different ring sizes: ligand specificities of the RGD-directed integrins. Biotechnology (N Y). 1995;13:265-270.
34. Pasqualini R, Arap W. Profiling the molecular diversity of blood vessels. Cold Spring Harb Symp Quant Biol. 2002;67:223-225.
35. Bhagwat SV, Petrovic N, Okamoto Y, Shapiro LH. The angiogenic regulator CD13/APN is a transcriptional target of Ras signaling pathways in endothelial morphogenesis. Blood. 2003;101:1818-1826.
36. Dixon J, Kaklamanis L, Turley H, et al. Expression of aminopeptidase-n (CD 13) in normal tissues and malignant neoplasms of epithelial and lymphoid origin. J Clin Pathol. 1994;47:43-47.
37. Colombo G, Curnis F, De Mori GM, et al. Structure-activity relationships of linear and cyclic peptides containing the NGR tumor-homing motif. J Biol Chem. 2002;277:47891-47897.
38. Bevers EM, Rosing J, Zwaal RF. Development of procoagulant binding sites on the platelet surface. Adv Exp Med Biol. 1985;192:359-371.
39. Dachary-Prigent J, Toti F, Satta N, Pasquet JM, Uzan A, Freyssinet JM. Physiopathological significance of catalytic phospholipids in the generation of thrombin. Semin Thromb Hemost. 1996;22:157-164.
40. Ortel TL, Quinn-Allen MA, Charles LA, Devore-Carter D, Kane WH. Characterization of an acquired inhibitor to coagulation factor V. Antibody binding to the second C-type domain of factor V inhibits the binding of factor V to phosphatidylserine and neutralizes procoagulant activity. J Clin Invest. 1992;90:2340-2347.